# Synthesis and Characterization of Cu-Co Substituted Strontium Hexaferrite for Magnetic Applications

**Burcu ERTUG** *

*İstanbul Bilgi University, Faculty of Engineering and Natural Sciences, Eski Silahtarağa Elektrik Santralı, Kazım Karabekir Cad., No: 2/13 34060 Eyüpsultan, Istanbul*

http://doi.org/10.5755/j02.ms.36798

*Received 27 March 2024; accepted 1 August 2024*

In this study, the structural and magnetic characterizations of a series of $SrCo_xCu_xFe_{12-2x}O_{19}$; $0.0 \leq x \leq 0.5$ samples, which were produced by the conventional ceramic method, were carried out. The structure was examined by X-ray diffraction (XRD) technique and optical microscopy. A vibrating sample magnetometer (VSM) was used to characterize the ferrimagnetic properties. XRD patterns confirmed the presence of a single phase as Sr-hexaferrite while there were not any peaks of unreacted $Fe_2O_3$ phase. The densities varied between 92 – 98 %. XRD patterns of the Sr-hexaferrite samples were slightly modified because of the co-substitution of Cu-Co; however, the magnetic properties changed remarkably. The sample with Cu-Co of $x = 0.1$ content had the highest saturation magnetization (33.52 emu/g), remanence (19.74 emu/g), and coercivity (4.3 kOe). The synthesized magnetic samples were found to be suitable for the development of attractive ferrimagnetic properties for the current ferrite magnets.
*Keywords:* hexaferrite, ferrimagnet, co-substitution.

## 1. INTRODUCTION

The development of thermal biology, bioengineering, and physics has led to a contribution to the hyperthermia treatment of cancer. The damage due to heating causes cancer cells to go through apoptosis. By the application of hyperthermia, microthrombosis forms in the capillary veins that feed the tumor, which prevents the feeding of it [1]. Under the alternating magnetic field, with the help of hysteresis losses, the magnetic materials placed inside the tumor produce the required heat to damage the cancer tissue [2]. By this process, tumor tissue is effectively heated and the local temperatures are adjusted to the range of 42 – 45 °C, and tumor tissue is selectively destroyed [3]. The candidate materials for this application are those containing $Fe_2O_3$ and showing ferrimagnetic behaviour and they are utilized as thermoseeds in the region to be treated [2, 4, 5].

In the few last decades, ferrimagnetic ceramics have become an attractive research field because they exhibit magnetic properties such as high Curie temperature, high saturation magnetization, magnetocrystalline anisotropy, etc. Several magneto-electric properties of these ceramics have led to the usage of them in different technological applications [6]. These hard ferrite ceramics are used as permanent magnets for generators, relays, and engines [7].

In the ionically bonded solids such as ferrimagnetic materials, a net magnetic moment is formed due to the antiparallel configuration of the magnetic dipoles of the different ions under the magnetic field [7].

The most important ferrite in this group is the barium ferrite ($BaFe_{12}O_{19}$) which was commercialized by Philips company with the name Ferroxdure in 1952. These materials are wet-pressed under the magnetic field to align the easy magnetization axis parallel to the applied magnetic field. The density and the cost of the hexagonal ferrites are low and their coercive force is high [8, 9].

The permanent magnets with the hexagonal barium and strontium ferrites are based on the magnetoplumbite structure. Strontium hexaferrites are known to exhibit a high Curie temperature in addition to excellent chemical stability and mechanical hardness. They are also appropriate candidates as high density magnetic recording media [10].

In the crystal structure of hexaferrites, there are 2 strontium cations, 24 iron, and 38 oxygen anions. Here, 24 iron cations occupy five crystal sites: 2a, 2b, 4f1, 4f2, and 12k. The spins of the $Fe^{3+}$ cations are parallel to the c-axis for the 2a (↑), 2b (↑), and 12k (↑) sites, while for the 4f1 (↓) and 4f2 (↓) sites they are opposite to the c-axis [11]. M-type hexaferrites are produced by the conventional ceramic route since that this route is both cost-effective and it is suitable for mass production [12].

The cation substitution technique has been extensively used by researchers to improve the performance of the M-type hexagonal ferrites [13]. These studies include Islam et al., (2024)'s Cu-Gd [14]; Idrees et al., (2022)'s Cu-Yb [15]; Rambabu et al., (2021) [16] Cu-La researches, that investigated the effect of copper together with a rare-earth element. Anantharamaiah et al., (2020) [17] focused on only the effect of Cu on the magnetic properties of Sr-hexaferrite whereas Rambabu et al., (2024) [18] worked on the effect of Cu-Ni along with La. This was one of the few studies which used two transition metals in their study. On the other hand, various studies focused on the single effect of cobalt substitution on the magnetic properties of Sr-hexaferrite [19 – 22]. Some researchers worked on the effect of two dopants such as Co-Mg [23] and Co-Ru [24]. Among the most recent researches on the Sr-hexaferrites, few studies

* Corresponding author. Tel.: +90-212-3115000.
E-mail: *burcu.ertug@bilgi.edu.tr* (B. Ertug)

focused on the effect of two transition metals together on the magnetic properties such as the one study on Co-Cr [25].

Considering there is a limited number of researches that cover the effect of two transition metals on the ferrimagnetic behaviour of strontium hexaferrites among the most recent studies, the purpose of this study is to investigate the effects which might be induced by the substitution of two divalent transition cations in strontium hexaferrite and the resultant magnetic properties. Two different species of divalent ions are selected, which are nonmagnetic cobalt- and copper-cations for $Fe^{3+}$ substitution in the Sr-hexaferrite.

## 2. EXPERIMENTAL DETAILS

### 2.1. Synthesis of the samples

$SrCo_xCu_xFe_{12-2x}O_{19}$; $0.0 \leq x \leq 0.5$ were produced by the standard ceramic method. The stoichiometric proportion of strontium carbonate (Chem-pure, Aromel Kimya), alfa-$Fe_2O_3$ (98 wt.%, ZAG Kimya), CuO (99 wt.%, Emir Kimya) and $Co_2O_3$ (99 wt.%, particle size below 44 μm, Nanokar) powders were used as the starting materials. Each powder batch was prepared as 3 g. In order to prevent the agglomeration, stearic acid was used in the mixture. The molar ratio of $Fe^{3+}$ to $Sr^{2+}$ was taken as 12:1. The codes SF-1, SF-2, SF-3, SF-4, and SF-5 were given to the samples, respectively. To obtain a homogeneous mixture, an agate mortar was used to mix the starting powders for sufficient time. The powder mixtures were pressed into pellets (diameter of 10 mm, thickness of 3 mm) by using an uniaxial pressing machine under a pressure of 60 kN/cm$^2$. The compacted samples were then sintered under an air atmosphere at 1250 ºC for 3 h. using the electrical furnace. After sintering, these samples were cooled to room temperature. The process diagram of the study is shown in Fig. 1.

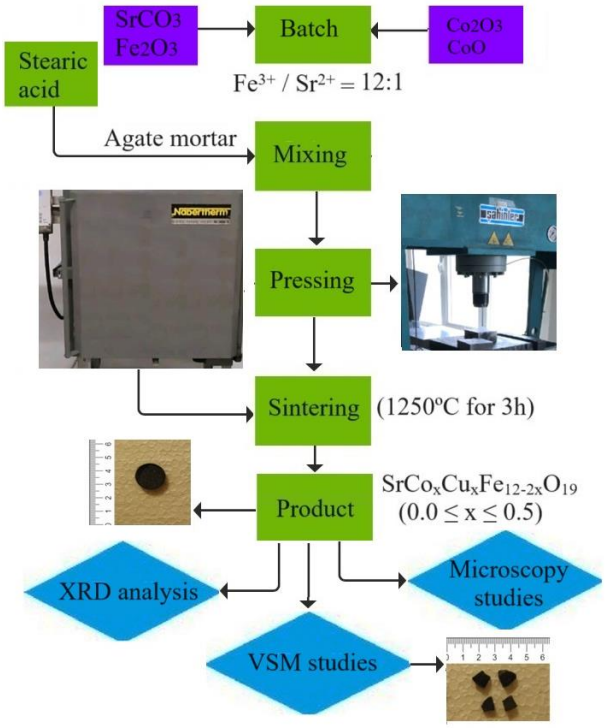


**Fig. 1.** The process diagram of the study

### 2.2. Characterization of the samples

#### 2.2.1. XRD studies

X-ray diffractometer (Rigaku D-Max2200) was used to identify the present phases of the samples using Cu-Kα radiation ($\lambda$ = 1.5418 Aº) in the 2Θ range of 20 – 70º.

The lattice parameters (a, c) of the as-sintered samples were estimated with the help of Bragg's law and using Eq. 1 below:

$$\frac{1}{d^2} = \frac{4}{3}.\frac{h^2+h.k+k^2}{a^2} + \frac{l^2}{c^2}, \quad (1)$$

where *d* is the plane spacing and (*hkl*) are the indices which belong to the diffraction planes.

#### 2.2.2. Density determination and optical microscopy

Also, the physical properties of the Sr-hexaferrite samples, such as as-sintered densities were calculated using the bottle pcynometer method using the Archimedes principle. The theoretical density of the strontium hexaferrite is 5.10 g/cm$^3$ [26]. The relative density and bulk density values were calculated and shown in Table 1. The surface preparation was applied to the as-sintered samples through polishing using SiC paper. Optical microscopy was used to observe the microstructural properties of the hexaferrites at different magnifications.

#### 2.2.3. Magnetic characterization of the hexaferrites

The magnetic characterization studies of the hexaferrites were carried out using vibrating sample magnetometry (Dexing Magnet VSM 550) by applying a maximum magnetic field of 10 kOe. The magnetization as a function of magnetic field (M-H) plots was drawn at room temperature.

## 3. RESULTS AND DISCUSSION

The density and porosity results after the sintering at 1250 °C for 3 h are tabulated in Table 1. As can be seen from the table, the relative density percentages were quite high, which implies that the samples were nearly sintered to full density and the sintering conditions were sufficient for the sintering.

**Table 1.** Relative density and porosity of the samples for different values of x

| Code | Sample | Sintering parameters | Density, g/cm$^3$ | Relative density, % | Porosity, % |
|---|---|---|---|---|---|
| SF1 | x = 0.1 | 1250ºC/3h | 4.7 | 92 | 8.0 |
| SF2 | x = 0.2 | 1250ºC/3h | 5.0 | 98 | 1.4 |
| SF3 | x = 0.3 | 1250ºC/3h | 4.7 | 93 | 6.7 |
| SF4 | x = 0.4 | 1250ºC/3h | 5.0 | 97 | 3.4 |
| SF5 | x = 0.5 | 1250ºC/3h | 4.7 | 93 | 6.6 |

The lowest relative density was around 92 %, it was obtained for the SF1 sample which contains 0.1 wt.% of Co and 0.1 wt.% Cu addition in the composition of Sr-hexaferrite compound. The highest relative densities were around 98 % and 97 % and they were found for SF2 and SF4 samples with 0.2 wt.% of and 0.4 wt.% of Co and Cu additions, respectively.

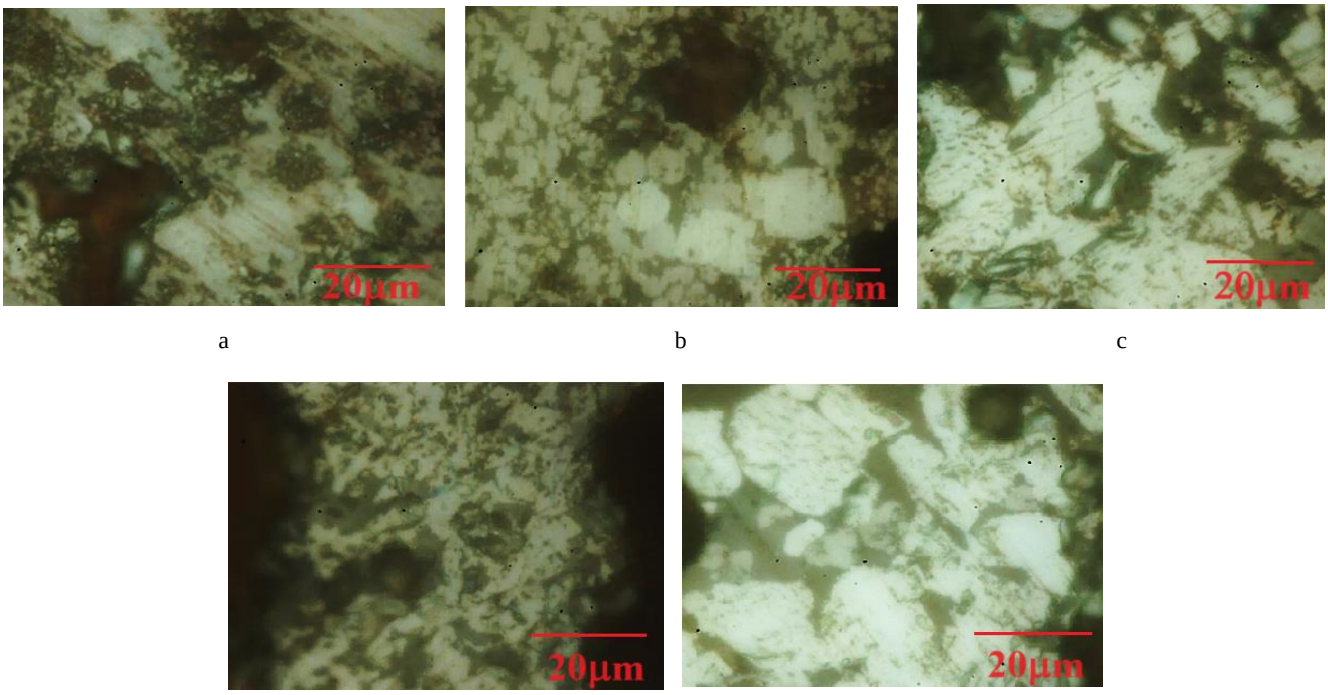


**Fig. 3.** Optical images of the samples at 1kx magnification: a – SF1; b – SF2; c – SF3; d – SF4; e – SF5

These two samples also exhibited sufficient mechanical integrity as they are dense hexaferrite samples (with a relative density of over 85 %).

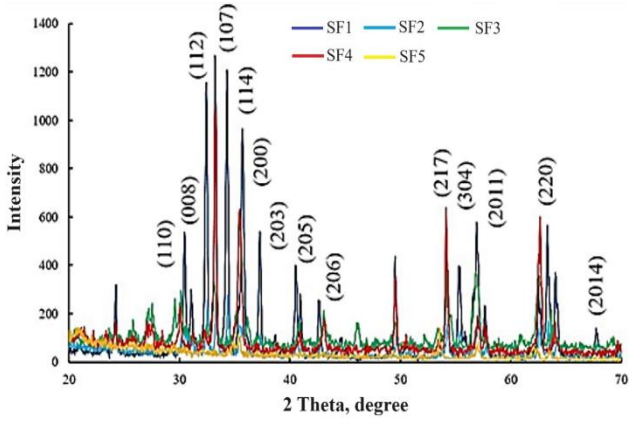


**Fig. 2.** XRD patterns of the substituted Sr-hexaferrite samples

XRD diffraction patterns of the studied samples are shown in Fig. 2. Bragg's peaks of the obtained patterns are in good agreement with the standard diffraction pattern [27] of the base material of $SrFe_{12}O_{19}$. Fig. 2 confirms the formation of the single-phase magnetoplumbite structure without showing any peaks of unreacted impurity phases.

The diffraction peaks that correspond to diffraction planes of (112), (107), (114), (200) and (217) are also presented in Fig.2. Since there was a substitution of Co and Cu cations in the magnetoplumbite structure, a slight change in the diffraction peak intensities and angle positions was observed. This can be attributed to the slight changes in the lattice parameters of the Sr-hexaferrite.

It was determined that the lattice parameter, *c* of $SrCo_xCu_xFe_{12-2x}O_{19}$ was 10.4 Å, and value of *a* was calculated to be 4.9 Å on average.

Optical images as in Fig. 3 were used to investigate the morphology in the $SrCo_xCu_xFe_{12-2x}O_{19}$ samples. According to the optical microscopy examinations, all samples consisted of particles of similar size. It was observed that there was not a noticeable change in the morphology when substituted with Cu-Co as demonstrated by the images. In all of the samples studied, the majority of the particles exhibited a size range of 23 – 25 µm. These particles were much larger than the critical domain size of the nanoscale.

As the sum of Cu and Co substitution increased, the hard ferrimagnetic behaviour exhibited by the SF1 and SF2 samples was replaced by soft ferrimagnetism, which is characterized by the reduction of the area of the hysteresis loss.

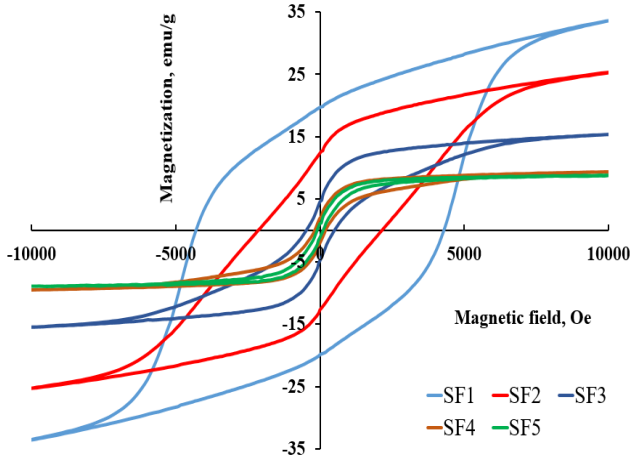


**Fig. 4.** Magnetization curves for Sr-hexaferrites

This behaviour was exhibited by the SF3, SF4 and SF5 samples, which contain 0.3 %, 0.4 % and 0.5 % of Co-Cu. In accordance with this result, the corresponding energy product, BHmax values of the SF3, SF4, and SF5 samples

were negligible. When the composition changed in terms of the amount of Co and Cu, the hard magnetic properties were reduced as a function of the amount of Sr-ferrite. The saturation magnetization (Ms) values of $SrCo_xCu_xFe_{12-2x}O_{19}$; ($0.0 \leq x \leq 0.5$) samples were calculated by M-H loops as shown in Fig. 4.

Fig. 4 indicates that there was a lack of saturation in the SF1 and SF2 samples, which was in accordance with a high coercivity and a wide ferrimagnetic loop. This is because of the large magnetocrystalline anisotropy. The saturation magnetization (*Ms*), remanence (*Mr*), squareness ratio (*Mr*/*Ms*) and coercivity (*Hc*) were determined by the hysteresis loops and were given in Table 3.

**Table 3.** Saturation magnetization (*Ms*), remanence (*Mr*), coercivity (Hc) of $SrCo_xCu_xFe_{12-2x}O_{19}$ samples

| Sample | *Ms*, emu/g | *Mr*, emu/g | *Mr*/*Ms* | *Hc*, Oe | *BH*max, kJ/m$^3$ |
|---|---|---|---|---|---|
| x = 0.1 | 33.52 | 19.74 | 0.62 | 4300 | 18.62 |
| x = 0.2 | 28.10 | 13.77 | 0.48 | 1850 | 10.35 |
| x = 0.3 | 18.83 | 7.59 | 0.33 | 157 | 2.60 |
| x = 0.4 | 12.70 | 3.20 | 0.20 | 155 | NA* |
| x = 0.5 | 8.62 | 1.92 | 0.36 | 95 | NA* |

Cu-Co substituted hexaferrites exhibited the saturation magnetization values from 33.52 emu/g at x = 0.1 to 18.83 emu/g at x = 0.3 and then dropped to 8.62 emu/g at x = 0.5. The coercivity values of Co-Cu substituted samples decreased from 4300 Oe at x = 0.1 to 1850 Oe at x = 0.3 and decreased further at higher concentrations of substituents. The coercivity value of SF1 was 4300 Oe, which is typical of hard ferrites. These hard ferrites are suitable as permanent magnets since their saturation magnetizations are relatively high. In a recent research, at a substitution level of x = 1.0, the coercivity values of Co-Sn and Zn-Sn samples were 1040 Oe and 1180 Oe, respectively [28]. The highest squareness value, SQR (Mr/Ms) was measured to be 0.62 and it was obtained from the SF1 sample, which implies that this sample could be a candidate for permanent magnets.

As the sum of Cu and Co substitution increased, the hard ferrimagnetic behaviour exhibited by the SF1 and SF2 samples was replaced by soft ferrimagnetism, which is characterized by the reduction of the area of the hysteresis loss. This behaviour was exhibited by the SF3, SF4 and SF5 samples, which contain 0.3 %, 0.4 %, and 0.5 % of Co-Cu. In accordance with this result, the corresponding energy product, BHmax values of the SF3, SF4, and SF5 samples were negligible.

**Table 4.** Comparison of several magnetic parameters of Sr-hexaferrites

| Substitution | *Ms*, emu/g | *Mr*, emu/g | *Mr*/*Ms* | *Hc*, Oe | Reference |
|---|---|---|---|---|---|
| Cr | 36.47 | 19.41 | 0.532 | 4490 | [6] |
| Fe-Sc | 31 | 16.8 | 0.54 | 1250 | [29] |
| Nano | 44.19 | 27.71 | 0.627 | 6403 | [30] |
| Cd-Co-Fe | 37.36 | 2.21 | 0.059 | 42.58 | [31] |
| C-Fe | 30 | NA (low) | - | 48 | [32] |
| Cu-Co | 33.25 | 3.33 | 0.10 | 117 | [33] |
| Cu-Co | 33.52 | 19.74 | 0.59 | 4300 | Present study |

When the composition changed in terms of the amount of Co and Cu, the hard magnetic properties were reduced as a function of the amount of Sr-ferrite. The saturation magnetization (*Ms*) values of $SrCo_xCu_xFe_{12-2x}O_{19}$; ($0.0 \leq x \leq 0.5$) samples were calculated by M-H loops as shown in Fig.4.

The highest BHmax values of SF1 and SF2 samples were calculated to be 18.62 and 10.35 kJ·m$^{-3}$, respectively (2.34 and 1.3 MGOe). The relevant results of the previous resarches on the several hexaferrites are given in Table 4. It was noted that several substitutions were used for the hexaferrites among which there were Cr, Cd, Cu, Co, Sc, and Fe with the corresponding ferrimagnetic responses [6, 29 – 33].

## 4. CONCLUSIONS

In this study, a series of $SrCo_xCu_xFe_{12-2x}O_{19}$ (x = 0.0, 0.1, 0.2, 0.3, 0.4, 0.5) were successfully synthesized by conventional ceramic method and sintered at 1250 ºC for 3 hours. As-sintered samples were densified to a level of 92 – 98 %. XRD patterns showed that all of the samples contained Sr-hexaferrite crystals as the only phase. The magnetic behaviour changed from hard ferrimagnetism to soft one with increasing Cu-Co co-substitution. This was because of the co-substitution of $Cu^{2+}$-$Co^{2+}$ for $Fe^{3+}$ at different contents (x = 0 – 0.5). The magnetization loops of the samples with Cu-Co of x = 0.3, 0.4, and 0.5 showed that the soft ferrimagnetism was present as evident from the reduction of the hysteresis loss. The highest saturation magnetization (33.52 emu/g) was obtained in the sample with Cu-Co of x = 0.1 content. The coercivity values of the samples varied drastically with different substitution levels, which can be explained by the differences in the crystal size. The highest coercivity was also found in the sample with Cu-Co of x = 0.1 content and it was 4.3 kOe. The squareness ratio, (Mr/Ms) varied between 0.36 – 0.62. The highest BHmax value was measured to be 18.62 kJ/m$^3$ and this was observed for the sample with Cu-Co content of x = 0.1. We suggest that the obtained results may open a new way for the development of attractive ferrimagnetic properties for the current ferrite magnets.


### *Acknowledgments*

The author acknowledges Afyon Kocatepe University, Department of Metallurgical and Materials Engineering, Afyon, for providing technical opportunities for this research work. The author is thankful to Metallurgical Engineer Haluk Gürses from Dokuz Eylül University, Department of Metallurgical and Materials Engineering, İzmir and EMUM Electronic Materials Production Laboratory for the XRD studies and the magnetic characterization, respectively.


### REFERENCES


1. Memorial Hospitals Group 2024: https://www.memorial.com.tr/hipertermi/
2. **Vincenzini, P.** Ed. Ceramics in Clinical Applications. Elsevier. Amsterdam. The Netherlands. 1987.
3. **Abdel-Hameed, S.A.M., Marzouk, M.A., Elwan, R.L.** In Vitro Evaluation of Some Types of Ferrimagnetic Glass-

ceramics *International Journal of Biomaterials* 2014: pp. 1 – 10. https://doi.org/10.1155/2014/415854

4. **Kokubo, T., Ito, S., Shigematsu, M., Sakka, S., Yamamuro, T.** Mechanical Properties of a New Type of Apatite-Containing Glass-Ceramic for Prosthetic Application *Journal of Materials Science* 20 (6) 1985: pp. 2001 – 2004. https://doi.org/10.1007/BF01112282
5. **Akao, M., Aoki, H., Kato, K.** Mechanical Properties of Sintered Hydroxyapatite for Prosthetic Applications *Journal of Materials Science* 16 (3) 1981: pp. 809 – 812. https://doi.org/10.1007/BF00552220
6. **Ghzaiel, T.B., Dhaoui, W., Pasko, A., Mazaleyrat, F.** Effect of Non-Magnetic and Magnetic Trivalent Ion Substitutions on Bam-Ferrite Properties Synthesized by Hydrothermal Method *Journal of Alloys and Compounds* 671 2016: pp. 245 – 253. https://doi.org/10.1016/j.jallcom.2016.02.071
7. **Smith, W.F.** Principles of Materials Science and Engineering. Mcgraw Hill Series In Materials Science and Engineering. 1990.
8. **Kools, F.** Hard magnetic ferrites, Concise Encyclopedia of Advanced Ceramic Materials. Pergamon 1991: pp. 200 – 206.
9. **Went, J.J., Rathenau, G.W., Gorter, E.W., Van Oosterhout, G.W.** Ferroxdure, a Class of New Permanent Magnet Materials *Phillips Technical Review* 13 (7) 1952: pp. 194 – 208.
10. **Borkar, B.T., Borkar, A.B., Janardhanan, D., Deshmukh, P., Thakare, P., Damodare, L.P., Choubey, S.R.** Lanthanum ($La^{3+}$) Substitution for $Fe^{3+}$ in Ba-Sr-Ca M-Type Hexaferrites and Their Synthesis and Characterization *European Journal of Materials Science and Engineering* 5 (1) 2020: pp. 3 – 10. https://doi.org/ 10.36868/ejmse.2020.05.01.003
11. **Ashraf, G.A., Zhang, L., Abbas, W., Murtaza, G.** Magnetic and Optical Properties of Gd-Tl Substituted M-Type Barium Hexaferrites Synthesized by Co-Precipitation Technique *Current Applied Physics* 19 2019: pp. 506 – 515. https://doi.org/ 10.1016/j.cap.2019.02.005
12. **Verma, S., Pandey, O.P., Paesano, A., Sharma, P.** Comparison of Structural and Magnetic Properties of $La^{3+,}$ Substituted $Bafe_{12}o_{19}$, Prepared by Different Substitution Methods *Physica B: Condensed Matter* 448 2014: pp. 57 – 59. https://doi.org/ 10.1016/j.physb.2014.03.035
13. **Lee, K., Kang, Y.M., Yoo, S.I.** Effects of La-Co Substitution and Post-Annealing on the Magnetic Properties of Srm Hexaferrites *SSRN* 2022: pp. 1 – 20. https://doi.org/10.2139/ssrn.4220774
14. **Islam, R., Khan, M.K.R., Hossain, S., Rahman, M.M., Haque, M.M., Aliuzzaman, M., Alam, M.K., Sarker, M.S.I.** Structural, Thermodynamic, and Magnetic Properties of $SrFe_{12}O_{19}$ Hexaferrite Modified by Co-Substitution of Cu and Gd *RSC Advances* 14 (11) 2024: pp. 7314 – 7328. https://doi.org/10.1039/d3ra08878b
15. **Idrees, M., Abbas, F., Sadiq, I., Khan, H.M., Sadiq, F., Nadeem, M., Hussain, S., Riaz, S., Naseem, S.** Theoretical and Experimental Investigations: Synergetic Effect of Yb–Cu Substitution on Different Properties of Hexagonal Ferrites *Journal of Physics and Chemistry of Solids* 170 2022: pp. 110904. https://doi.org/10.1016/j.jpcs.2022.110904
16. **Rambabu, Ch., Subrahmanya, S.K., Shivanarayana, Ch., Padmavathi, U., Swetha, R., Raju, M.K., Batoo, K.M., Murali, N., Verma, R., Lakshminarayana, P.V.** Effect of La-Cu Co-Substitution on Structural, Microstructural and Magnetic Properties of M-type Strontium Hexaferrite (Sr1−xLaxFe12−xCuxO19) *Inorganic Chemistry Communications* 134 2021: pp. 109053. https://doi.org/10.1016/j.inoche.2021.109053
17. **Anantharamaiah, P.N., Sarath Chandra, N., Shashanka, H.M., Kumar, R., Sahoo, B.** Magnetic and Catalytic Properties of Cu-substituted $SrFe_{12}O_{19}$ Synthesized by Tartrate-gel Method *Advanced Powder Technology* 31 (6) 2020: pp. 2385 – 2393. https://doi.org/10.1016/j.apt.2020.04.004
18. **Rambabu, Ch., Aruna, B., Shanmukhi, P.S.V., Kiran, M.G., Murali, N., Mammo, T.W., Parajuli, D., Choppara, P., Himakar, P., Narayana, P.V.L.** Effect of $La_3$+/$Cu_2$+ and $La_3$/$Ni_2$+ Substitution on the Synthesis, Magnetic and Dielectric Properties of M−type Sr1-xLaxFe12-xMxO19 (M =c Cu and Ni) Hexaferrite *Inorganic Chemistry Communications* 159 2024: pp. 111753. https://doi.org/10.1016/j.inoche.2023.111753
19. **Alipour, A., Torkian, Sh., Ghasemi, A., Tavoosi, M., Gordani, G.R.** Magnetic Properties Improvement Through Exchange-coupling in Hard/Soft $SrFe_{12}O_{19}$/Co Nanocomposite *Ceramics International* 47 (2) 2021: pp. 2463 – 2470. https://doi.org/10.1016/j.ceramint.2020.09.089
20. **Lamouri, R., Daoudi, K., Absike, H., Mounkachi, O., Salmani, E., Hamedoun, M., Benyoussef, A., Ez-Zahraouy, H.** Structural, Electronic and Magnetic Properties of Co-substituted $SrFe_{12}O_{19}$: A DFT Study *Materials Today Communications* 28 2021: pp. 102589. https://doi.org/10.1016/j.mtcomm.2021.102589
21. **Nguyen, H.H., Tran, N., Phan, T.L., Yang, D.S., Dang, N.T., Lee, B.W.** Electronic Structure, and Magnetic and Microwave Absorption Properties of Co-doped $SrFe_{12}O_{19}$ Hexaferrites *Ceramics International Part B* 46 (11) 2020: pp. 19506 – 19513. https://doi.org/10.1016/j.ceramint.2020.04.304
22. **Abdel Hakeem, A.M., Ibrahim, E.M.M., Ali, H.M., Shokr, E.Kh., Hamazaoui, A., Ahmed, M.R.** Dielectric, Magnetic and Structural Properties of Co-doped Hexaferrite Synthesized by Microwave Digestion System *Journal of Alloys and Compounds* 872 2021: pp. 159669. https://doi.org/10.1016/j.jallcom.2021.159669
23. **Sriramulu, G., Praveena, K., Ravinder Reddy, B., Kandasami, A., Katlakunta, S.** Observation of Rhombohedral $CoFe_2O_4$ Phase in Co-Mg Co-doped $SrFe_{12}O_{19}$ Hexaferrite *Journal of Magnetism and Magnetic Materials* 583 2023: pp. 171046. https://doi.org/10.1016/j.jmmm.2023.171046
24. **Meng, C., Chang, Y., Zhang, Y., Liu, S., Chang, H.** Structural, Electromagnetic Properties and Broad Microwave Absorption Bandwidth of $SrFe_{12-2x}Co_xRu_xO_{19}$ *Ceramics International* 46 (14) 2020: pp. 22338 – 22344. https://doi.org/10.1016/j.ceramint.2020.05.315
25. **Gupta, A., Roy, P.K.** Synthesis and Tuning the Electro-Magnetic Properties of Co-Cr Substituted Sr-hexaferrite Towards Diverse Usages *Materials Science and Engineering: B* 263 2021: pp. 114815. https://doi.org/10.1016/j.mseb.2020.114815
26. **Martina, E.G., Miralles, C.G., Gomez, S.R., Perez, L., Del Campo, A., Minguez, J.C.G., Fernandez, C.J., Quesada, A., Fernandez, J.F., Serrano A.,** Dense Strontium Hexaferrite-Based Permanent Magnet Composites

Assisted by Cold Sintering Process *Journal of Alloys and Compounds* 917 2022: pp. 165531. https://doi.org/10.1016/j.jallcom.2022.165531

27. **Agrawal, S., Parveen, A., Azam, A.** Room Temperature Optical and Dielectric Properties of Ca and Ni Doped Barium Ferrite *AIP Conference Proceedings* 1728 (1) 2016: pp. 020205. https://doi.org/10.1063/1.4946256
28. **Al-Garalleh, G.A., Mahmood, S.H., Bsoul, I., Loloee, R.** Structural and Magnetic Properties of RE-Al Substituted Nanocrystalline Hexaferrites ($Sr_{1-x}RE_xAl_2Fe_{10}O_{19}$) *Materials Research Express* 7 2020: pp. 026103. https://doi.org/10.1088/2053-1591/ab5ddd
29. **Belec, B., Drazi, G., Gyergyek, S., Podmiljšak, B., Goršak, T., Komelj, M., Nogués, J., Makovec, D.** Novel Ba-Hexaferrite Structural Variations Stabilized on the Nanoscale as Building Blocks for Epitaxial Bi-Magnetic Hard/Soft Sandwiched Maghemite/Hexaferrite/Maghemite Nanoplatelets with Out-Of-Plane Easy Axis and Enhanced Magnetization *Nanoscale* 2017: pp. 1 – 3. https://doi.org/10.1039/C7NR05894B
30. **Azis, R.S., Sulaiman, S., Ibrahim, I.R., Zakaria, A., Hassan, J., Muda, N.N.C., Nazlan, R., Saiden, N.M., Fen, Y.W., Mustaffa, M.S., Matori, K.A.** Influence of pH Adjustment Parameter for Sol-Gel Modification on Structural, Microstructure, and Magnetic Properties of Nanocrystalline Strontium Ferrite *Nanoscale Research Letters* 13 (160) 2018: pp. 1 – 13. https://doi.org/10.1186/s11671-018-2562-x
31. **Ali, I., Amin, N., Rehman, A., Akhtar, M., Fatima, M., Mahmood, K., Ali, A., Mustafa, G., Hasan, M.S., Bibi, A., Iqbal, M.Z., Iqbal, F., Aslam, A., Mehmood, K., Latif, Z., Hussain, K., Nawaz, Z.H., Sharif, S., Jilani, M., Danish, U., Yaseen, I., Dilbar, A., Tahir, N., Bilal, M., Amin, A., Arshad, M.I.,** Electrical and Magnetic Properties Of $BaCo_xCd_{2-x}Fe_{16}O_{27}$ W-Type Hexaferrites ($0 \leq x \leq 0.5$) *Digest Journal of Nanomaterials and Biostructures* 15 (1) 2020: pp. 67 – 73. https://doi.org/10.15251/DJNB.2020.151.67
32. **Koutzarova, T., Georgieva, B., Kolev, S., Krezhov, K., Kovacheva, D., Ghelev, C., Vertruyen, B., Boschini, F., Mahmoud, A., Tran, L.M., Zaleski, A.** Study of the Properties of Co-Substituted $Ba_2Mg_2Fe_{12}O_{22}$ Hexaferrites *The 3rd International Electronic Conference on Materials Sciences* 2018: pp. 1 – 7. https://doi.org/10.3390/ma12091414
33. **Mohammed, I., Mohammed, J., Kende, A.U., Wara, A.M., Aliero, Y.A., Magawata, U.Z., Umar, A.B., Srivastava, A.K.** Review on Y-type Hexaferrite: Synthesis, Characterization and Properties *Applied Surface Science Advances* 16 2023: pp. 100416. https://doi.org/10.1016/j.apsadv.2023.100416